

# INHIBITION OF GALVANIC CORROSION OF WNC BARRIER METAL FOR RELIABLE CU CMP

D. Ernur<sup>1,2</sup>, V. Terzieva<sup>1</sup>, J. Schuhmacher<sup>1</sup> and K. Maex<sup>1,2</sup>

<sup>1</sup> IMEC, Kapeldreef 75, B-3001 Leuven, Belgium,

<sup>2</sup> K. U. Leuven, ESAT, Kasteelpark Arenberg 10, 3001 Leuven, Belgium,

© 2004 Prepared for presentation at AIChE 2004 Annual Meeting/November 7-12/Interfacial Phenomena in Semiconductor Processing

AIChE Shall Not Be Responsible For Statements or Opinions Contained in Papers or Printed in its Publications.

## Abstract

This paper discusses chemical and galvanic corrosion of tungsten nitride carbide (WNC) barrier metal. Chemical corrosion occurs due to the oxidation of W in the WNC film by H<sub>2</sub>O<sub>2</sub>, which is used as oxidizer in CMP slurries, followed by the dissolution of the oxide complex. Galvanic corrosion takes place due to the high potential difference between Cu and WNC established in the presence of H<sub>2</sub>O<sub>2</sub> based slurries during the CMP process. Use of HNO<sub>3</sub> as the oxidizing agent instead of H<sub>2</sub>O<sub>2</sub> reduces chemical and galvanic corrosion of WNC. In order to protect Cu against corrosion in such model slurries organic acids are used as additives. Malic acid containing HNO<sub>3</sub> based corrosion inhibiting model slurry is further tested on an experimental CMP tool for wafer level tests that showed promising Cu and WNC compatibility.

## Introduction

Cu damascene process has been successfully adopted in order to integrate Cu in ultra large-scale integrated (ULSI) circuits due to its lower resistivity and high electromigration resistance compared to aluminium (Al) [Edelstein *et al.*, 1997]. Within the damascene architecture, chemical mechanical planarization (CMP) is technologically recognized for providing global planarization and defining the topography. However, reliability issues associated with the CMP process include erosion of the interlayer dielectric, surface defects, dishing and corrosion.

In the manufacturing of microelectronic devices corrosion occurs for many reasons. During CMP process different corrosion phenomena such as chemical corrosion, photo-corrosion, and narrow trench corrosion are reported to occur [Kondo *et al.*, 2000, Homma *et al.*, 2000, Ernur *et al.*, 2002]. *Galvanic corrosion* occurs when two dissimilar metals are in electrical and in ionic contact. It occurs during the CMP process where Cu and the barrier metal are in electrical contact and CMP slurry acts as the

electrolyte providing the ionic contact medium. The less noble side, either Cu or the barrier metal, behaves as the anode showing enhanced dissolution. The extent of galvanic corrosion depends on the polarization kinetics of the metals, the cathode/anode area ratio and the ohmic resistance.

Materials such as Ta, TaN, Ti, TiN, W, WNC have been investigated for their potential use as diffusion barriers. However, some are reported to be responsible for galvanic corrosion. Cu/Ta couple is shown to give rise to galvanic corrosion during the barrier polish step resulting in Ta oxidation and  $\text{Cu}^{+2}$  reduction leaving Cu nodules at the Cu/Ta interface [Miller et. al., 2001]. Ti dissolution is accelerated by  $\text{Cu}^{+2}$  ions [Steigerwald et. al., 1995]. Enhanced W etching during CMP is attributed to galvanic corrosion [Kondo et. al., 2000, Zeidler et. al., 1997], which can arise from the presence of  $\text{H}_2\text{O}_2$  in the slurry [Ernur et. al., March 2002].

This study reports on the investigation of chemical and galvanic corrosion of WNC barrier metal induced by  $\text{H}_2\text{O}_2$  based slurries. Use of  $\text{HNO}_3$  based organic acid containing model slurries is shown to reduce corrosion of WNC barrier metal. Based on our results, we suggest that barrier compatible slurry chemistry is required to establish a reliable Cu CMP process.

## Experimental

Blanket Cu wafers are obtained by depositing 25 nm thick Ta layer as the diffusion barrier, followed by depositing 150 nm thick Cu seed layer in a physical vapor deposition (PVD) chamber (Electra™) on 500 nm thick  $\text{SiO}_2$  deposited on 50 nm thick  $\text{Si}_3\text{N}_4$  substrate. The deposition of 1  $\mu\text{m}$  thick Cu layer is done in an electrochemical deposition (ECD) chamber (Semitool Equinox) with Nanoplate 2001 chemistry from Shipley Inc. Annealing is done ex-situ in a furnace (AST SHS 2800 Steag) at 200 °C under  $\text{N}_2$  atmosphere for 30 seconds. Partial CMP is performed in linear type polishing machine (Lam Teres) using a low abrasive slurry (C430-A18). 50 nm thick WNC barrier metal is deposited by atomic layer deposition (ALD) in an ALD chamber (ASM Pulsar<sup>R</sup> 2000) on a 500 nm thick plasma  $\text{SiO}_2$  deposited on 50 nm thick  $\text{Si}_3\text{N}_4$  substrate.  $\text{H}_2\text{O}_2$  based citric acid ( $\text{C}_6\text{H}_8\text{O}_7$ ) and malic acid ( $\text{C}_4\text{H}_6\text{O}_5$ ) containing model slurries and a commercial slurry are used to study the corrosion of WNC barrier metal. In order to reduce WNC corrosion  $\text{HNO}_3$  is used to replace  $\text{H}_2\text{O}_2$ , which helps to oxidize and etch Cu, in the formulation of the corrosion inhibiting model slurries. Organic acids such as citric acid, malic acid and acetic acid ( $\text{C}_2\text{H}_4\text{O}_2$ ), are additionally mixed to avoid anisotropic Cu etching by  $\text{HNO}_3$ , which leads to high roughness on the surface of Cu due to the high density of corrosion pits [Ernur et. al., 2002, Ernur et. al., 2003].

A 2x2 cm<sup>2</sup> area on Cu and WNC electrodes is exposed to the slurries contained in a 120 ml beaker. The electrodes are connected to each other through a digital multimeter (Keithley Model 195A), which is used to measure current change during the reaction. The experimental set-up is schematically given in Fig. 1.

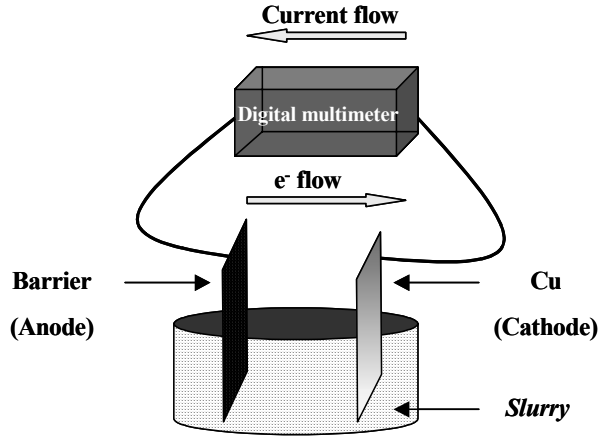


**Figure 1:** Schematics of the experimental set-up.

A Pt rod is used as the reference electrode to measure voltage using the same set-up. The samples are rinsed with de-ionized water (DI) after the reaction is completed and dried using a N<sub>2</sub> gun. Thickness loss ( $\Delta T$ ) in nanometers is calculated by measuring the sheet resistance before and after each experiment. X-Ray Fluorescence (XRF) analysis is performed to monitor the amount of W remaining in the WNC film. Transmission Electron Microscopy (TEM) and focused ion beam (FIB) analysis are used to monitor the Cu damascene structures after the CMP process is completed.

## Results and Discussions

### **Chemical and galvanic corrosion of WNC barrier metal**

Figure 2 presents a comparison of the change in WNC loss as a function of time after chemical dip and after galvanic coupling to Cu when H<sub>2</sub>O<sub>2</sub> based commercial and model slurries are used. The increase in WNC loss shows that these slurries remove the WNC barrier metal chemically. However, as a result of galvanic coupling to Cu, WNC loss is enhanced.

We suggest that the oxidation of W in WNC film by H<sub>2</sub>O<sub>2</sub> in the slurry and the dissolution of the oxide complex into the slurry results in WNC loss. Reaction of W with oxidizers in the slurry leads to the formation of a complex surface film.

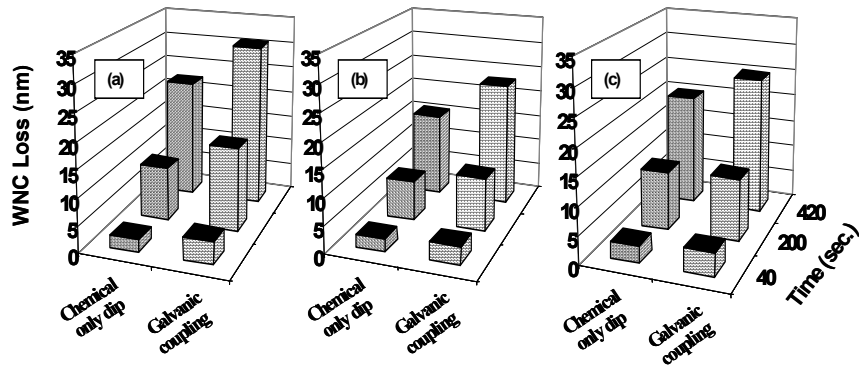


**Figure 2:** Comparison of WNC loss as a function of time after chemical dip and galvanic coupling using  $H_2O_2$  based (a) commercial slurry, (b) citric acid containing model slurry and (c) malic acid containing model slurry.

In many cases oxidation is reported to occur in two steps [Kneer et. al., 1997, Fauconnier and Vennereau, 1978].  $H_2O_2$  forms a non-stoichiometric  $WO_2/WO_3$  duplex oxide, which is soluble [Fauconnier and Vennereau, 1978]. Such a mechanism has also been the scope of modeling of W CMP [Paul, 2001]. Oxidation of W in the WNC film by  $H_2O_2$  and the dissolution of the oxide complex into the slurry results in WNC loss.

XRF spectrum given in Fig. 3 presents the amount of W remaining in the WNC film after chemical dip by using commercial slurry. With the increase in reaction time, the amount of W in WNC film decreases. This shows that WNC etching takes place through W loss.

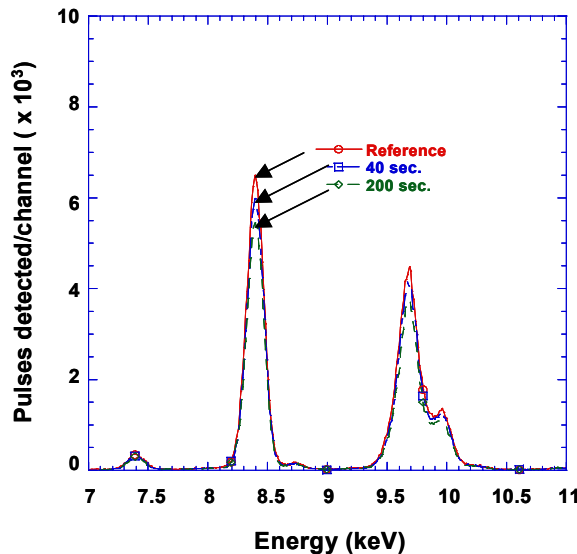


**Figure 3:** XRF spectrum of W remaining in WNC film after chemical dip using commercial slurry.

The enhancement in WNC loss as a result of galvanic coupling originates from the high potential difference between WNC and Cu in  $H_2O_2$

based slurries. This is illustrated in Table 1. When the potential difference between Pt-WNC couple is very large from that of Pt-Cu couple in slurry, it is highly likely to have galvanic coupling when Cu and WNC are coupled with each other in that slurry. In this respect, it is shown in Table 1 that the potential difference between Pt-Cu and Pt-WNC is the lowest when HNO<sub>3</sub> based model slurry is used.

**Table 1:** Potential difference between Pt-Cu and Pt-WNC couples in H<sub>2</sub>O<sub>2</sub> based commercial slurry and organic acid containing model slurries and HNO<sub>3</sub> based model slurry.

	$\Delta V$ (Pt-Cu) (mV)	$\Delta V$ (Pt-WCN) (mV)	emf (mV)
<b>Commercial Slurry</b>	-78.83	273.59	352.42
<b>Citric Acid Containing</b>	-52.46	188.15	240.61
<b>Malic Acid Containing</b>	-40.99	238.08	279.07
<b>HNO<sub>3</sub> Based</b>	515.03	597.9	82.87

Therefore, galvanic coupling is less likely to occur when Cu and WNC are brought into contact in this model slurry. This argument is supported by the low WNC loss with an etch rate value that is below 1 nm/min. On the other hand, the difference in potential between Pt-Cu and Pt-WNC is very high in H<sub>2</sub>O<sub>2</sub> based commercial slurry and organic acid containing model slurries. Therefore, while WNC behaves as the anode, Cu acts as the cathode. As a result, anodic dissolution of WNC leads to enhanced WNC loss in such slurries.

Figure 4 presents the current change as a function of time when H<sub>2</sub>O<sub>2</sub> based and HNO<sub>3</sub> based slurries are used. It is shown that H<sub>2</sub>O<sub>2</sub> based slurries show similar current behavior over time. However, commercial slurry results in almost two times increase in galvanic current in comparison to the organic acid containing model slurries. On the other hand, HNO<sub>3</sub> based model slurry presents very low current flow. This indicates weaker galvanic coupling between Cu and WNC barrier metal.

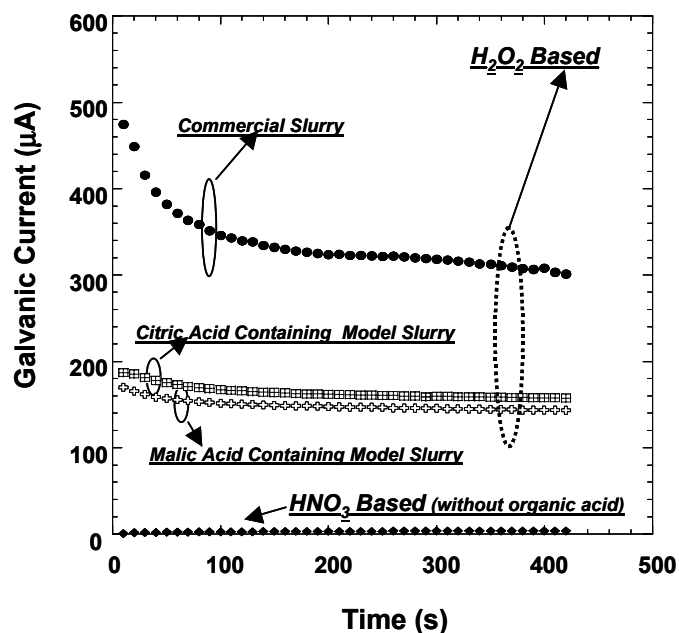


**Figure 4:** Current change as a function of time by using  $H_2O_2$  based and  $HNO_3$  based slurries

### Corrosion inhibition

Inhibition of galvanic corrosion depends on the choice of barrier metal and the slurry chemistry. In this respect, an amorphous metal such as WSiN shows good corrosion resistance [Iijima et. al., 1996]. On the other hand, WNC barrier metal is reported to have less severe galvanic corrosion in comparison to W barrier metal in  $H_2O_2$  based slurries due to the presence of  $-N$  and  $-C$  bonding [Ernur et. al., October 2002]. However, it still suffers from galvanic corrosion in such slurries. This draws the attention to the importance of slurry chemistry in order to reduce galvanic corrosion.

Figure 5 presents galvanic current change in the presence of  $HNO_3$  based corrosion inhibiting model slurries. Compared to the data given in Fig. 4 for  $H_2O_2$  based slurries, corrosion inhibiting model slurries result in very low current flow. This indicates reduction in galvanic coupling. Etch rate of WNC film by these corrosion inhibiting model slurries is determined to be less than 1 nm/min.

XRF spectrum given in Fig. 6 shows a comparison of the amount of W remaining in WNC film after galvanic coupling to Cu by using commercial slurry and  $HNO_3$  based malic acid containing corrosion inhibiting model slurry. Despite the fact that W amount decreases when commercial slurry is used, corrosion inhibiting slurry does not reveal significant W loss from WNC film.

Potential difference of Pt-Cu couple and Pt-WNC couple is given in Table 2. The fact that the value of potential difference of Pt-WNC couple is close to that of Pt-Cu couple in these model slurries unlike in commercial slurry, explains the reduction in galvanic corrosion of WNC barrier metal.

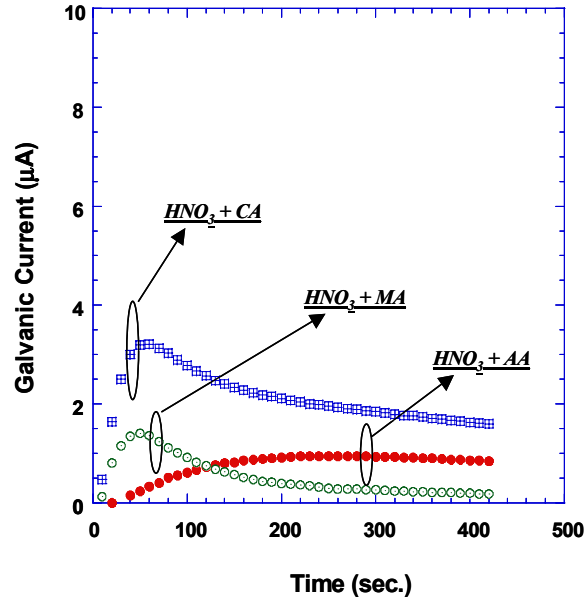


**Figure 5:** Current change as a function of time by  $\text{HNO}_3$  based organic acid containing corrosion inhibiting model slurries.

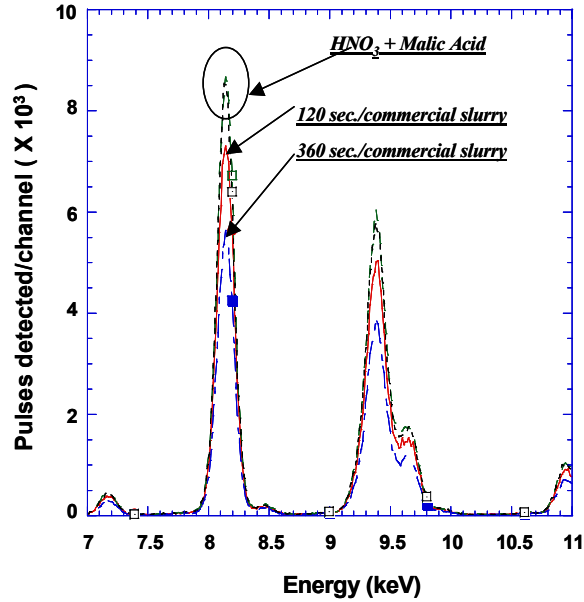


**Figure 6:** XRF spectrum of W remaining in the WNC film after galvanic coupling by using commercial slurry and  $\text{HNO}_3$  based malic acid containing corrosion inhibiting model slurry.

**Table 2:** Potential difference (mV)

	$\Delta V$ (Pt-Cu) (mV)	$\Delta V$ (Pt-WCN) (mV)	emf (mV)
HNO <sub>3</sub> + Citric Acid	629.63	640.25	11
HNO <sub>3</sub> + Malic Acid	595.96	625.23	29

Figure 7 demonstrates cross-section TEM and FIB images of Cu damascene lines after CMP process is completed. It is seen in Fig. 7 (a) that WNC barrier metal is lost in the top part of the trench sidewall at the interface with Cu when H<sub>2</sub>O<sub>2</sub> based commercial slurry is used. However, using HNO<sub>3</sub> based malic acid containing corrosion inhibiting model slurry reduces WNC loss from the corners of the trenches indicating reduction of galvanic coupling as shown in Fig. 7 (b).

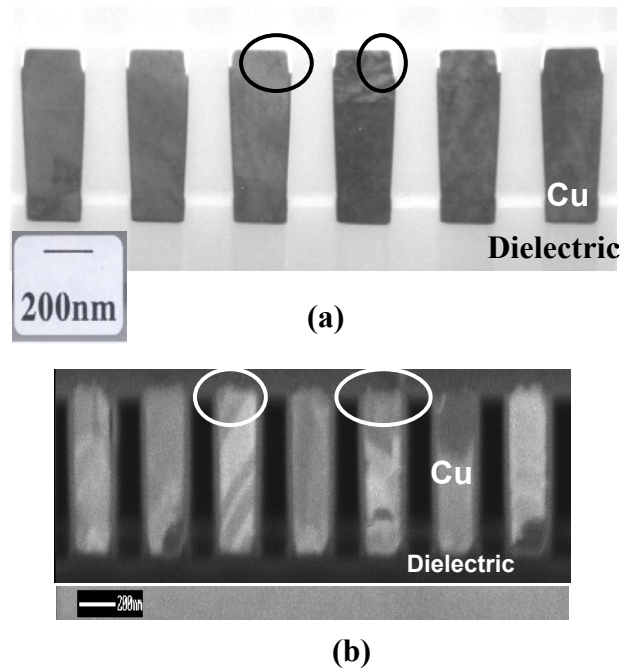


**Figure 7:** Cross section (a) TEM and (b) FIB images of Cu damascene lines with WNC barrier metal after CMP by using (a) H<sub>2</sub>O<sub>2</sub> based commercial slurry and (b) HNO<sub>3</sub> based malic acid containing corrosion inhibiting model slurry.

## Conclusions

Chemical and galvanic corrosion of WNC barrier metal is demonstrated to occur due to the presence of H<sub>2</sub>O<sub>2</sub> in CMP slurries. High potential difference between Cu and WNC barrier metal is responsible for galvanic corrosion that results in enhanced WNC loss. We offer the use of organic acid containing HNO<sub>3</sub> based model slurries to avoid chemical and galvanic



corrosion of WNC barrier metal. Our results draw the attention to the fact that slurry chemistry plays an important role in terms of galvanic corrosion and in terms of the reliability of the CMP process.

## References

- D. Edelstein, J. Heindenreich, R. Goldblatt, W. Cote, C. Uzoh, N. Lustig, P. Roper, T. McDevitt, W. Motsiff, A. Simon, J. Dukovic, R. Wachnik, H. Rathore, R. Schulz, L. Su, S. Luce and J. Slattery, "**Full Copper Wiring in a Sub-0.25 micro-m CMOS ULSI Technology**", *Proceedings of International Electron Devices Meeting (IEDM)*, 773 (1997).
- D. Ernur, S. Kondo and K. Maex, "**Narrow Trench Corrosion of Copper Damascene Interconnects**", *Jpn. J. Appl. Phys.*, **41**, (12), 7338 (2002).
- D. Ernur, S. Kondo, D. Shamiryman, and K. Maex, "**Investigation of barrier and slurry characteristics on the galvanic corrosion of copper**" *Microelectronic Engineering*, Vol. 64: (1-4) pp. 117-124, 2002. (MAM2002, Vaals, The Netherlands, March 3-6, 2002).
- D. Ernur, V. Terzieva, J. Schuhmacher, and K. Maex, "**Galvanic corrosion testing of  $WC_xN_y$  barrier metal in  $H_2O_2$  based slurries**", *Proc. of the Advanced Metallization Conf.*, pp. 95-101, 2002. (San Diego, CA, USA, October 1-3, 2002).
- D. Ernur, L. Carbonell, and K. Maex, "**The impact of annealing on the corrosion mechanism of copper films**", *Mechanisms in Electrochemical Deposition and Corrosion, MRS Symposium Proceedings*; Vol. 751E, pp. Z2.7, (Electronic-only publication) (San Francisco, CA, USA, April 21-25, 2003).
- J. Fauconnier and P. Vennereau, "**Comparison of formation kinetics of passivating layer of  $WO_3$  on (100) and (110) Oriented Tungsten Mono-Crystal Electrodes in  $H_2SO_4$  1M Medium**", *Electrochim. Acta*, **23**, 113 (1978).
- Y. Homma, S. Kondo, N. Sakuma, K. Hinode, J. Noguchi, N. Ogashi, H. Yamaguchi and N. Owada, "**Control of Photocorrosion in the Copper Damascene Process**", *J. Electrochem. Soc.*, **147**, (3), 1193 (2000).
- T. Iijima, Y. Shimooka, G. Minamihaba, T. Kawanoue, H. Tamura, H. Hirabayashi, N. Sakurai, H. Ohkawa, T. Kubota, Y. Mase, M. Koyama, J. Ooshima, J. Wada and K. Suguro, "**Microstructure and Electrical Properties of Amorphous W-Si-N Barrier Layer for Cu Interconnections**", *13<sup>th</sup> International VLSI Multilevel Interconnection Conference Proceedings*, (1996)
- E. A. Kneer, C. Raghunath, V. Mathew, S. Raghavan, and J. S. Leon, "**Electrochemical Measurements During the Chemical Mechanical Polishing of Tungsten Thin Films**", *J. Electrochem. Soc.*, **144**, 3041 (1997).

S. Kondo, N. Sakuma, Y. Homma and N. Ohashi, "**Slurry Chemical Corrosion and galvanic Corrosion During Copper Chemical Mechanical Polishing**", *Jpn. J. Appl. Phys.*, **39**, 6216 (2000).

A. E. Miller, P. B. Fischer, A. D. Keller and K. C. Cadien, "**Chemically Induced Defects During Copper Polish**", *International Interconnect Technology Conference (IITC) Proceedings*, 143-145 (2001)

E. Paul, "**Application of a CMP Model To Tungsten CMP**", *J. Electrochem. Soc.*, **148**, (6), G359-G363 (2001).

J. M. Steigerwald, S. P. Murarka, R. J. Gutmann and D. J. Duquette, "**Chemical Processes in the Chemical-Mechanical Polishing of Copper**", *Mat. Chem. And Phys.*, **41**, 217-228 (1995).

D. Zeidler, Z. Stavreva, M. Plotner and K. Drescher, "**Characterization of Cu Chemical Mechanical Polishing by Electrochemical Investigations**", *Microelectronic Engineering*, **33**, 259-265 (1997)